Reconstruction of the point spread function from ADONIS AO measurements: limits of the method and photometric accuracy*

Stephan Harder[1] and Alain Chelli[1]

[1] Laboratoire d'Astrophysique, Observatoire de Grenoble, BP 53,
F-38041, Grenoble Cedex 9, France
* Comments to: Stephan.Harder@obs.ujf-grenoble.fr

Abstract –

Wavefront correction by adaptive optics is often only partial and the image of a point-like source consists of a coherent peak superposed on a diffuse halo. If the point-spread function (PSF) is known, the object can be restored by deconvolution techniques. This PSF depends, however, strongly on atmospheric conditions which are variable and on the wavefront sensor reference source. For this reason, the image of a point-like source does not always fit well the PSF at the time of the object acquisition. It is thus important to estimate the PSF simultaneously with the observation of the object. Recently, we have reported on our first results of PSF reconstruction on a bright reference source, observed with the adaptive optics system *ADONIS*. We now present results on faint reference sources observed under bad seeing conditions. We discuss the limits of the reconstruction method for both cases and find that a variable residual aberration which we interpret in terms of a local turbulence can at least partly explain the error on the PSF reconstruction. From simulations, we studied the conservation of the flux ratio of double systems when using the reconstructed PSF as calibrator in deconvolution. It is shown that for flux ratios up to 2 the mean relative error on the flux ratio estimate is about 2-3%, while it is about 7% for flux ratios of 4 and 25% for higher flux ratios. The same errors are found, when using the image of a point-like source observed 30 min later as PSF calibrator.

1 Introduction

The point-spread function (PSF) in adaptive optics (AO) is very variable, since it depends highly on atmospheric conditions like seeing and the characteristics of the reference source like magnitude. This makes it difficult to calibrate the PSF by observing a point-like source as it is usually done by AO observers. A good PSF estimation is important to improve the quality of the image by deconvolution techniques in order to do accurate photometry or to detect faint structures. A solution to this dilemma may be found, if the PSF can be estimated from the wavefront sensor measurements and AO control loop data saved during the object acquisition.

The feasibility of this approach has been shown by Veran et al. ([6]) who developed a method to reconstruct the PSF from AO control loop data and an accurate model of the atmospheric turbulence. They successfully applied this method to the AO system *PUEO* installed at the 3.6m telescope of *CFHT* at Mauna Kea. However, it remains to show the validity of the method to other AO systems, in particular those which do not use a curvature sensor, but a Shack-Hartmann wavefront sensor. We have started to apply the reconstruction method to *ADONIS,* which is the AO system at the 3.6m ESO telescope at La Silla. It is a system based on a Shack-Hartmann sensor with 7×7 subapertures and which corrects 50 modes. The deformable mirror consists of a mirror with piezo-stack elements and a separated plan mirror to do the tip/tilt correction.

In a previous publication ([3]), we presented first results of the PSF reconstruction for *ADONIS.* The results were very promising, since the observed and estimated Strehl ratios were similar and since the observed and estimated optical transfer functions differed less than 10 to 20 % from each other. However, a residual aberration with the form of a triangular coma seen in the long-exposure image cannot be modeled by the PSF reconstruction method. This aberration is variable in time and non centro-symmetric and is probably due to the presence of a local turbulence, e.g. situated above the primary mirror.

We give a brief summary of the reconstruction method in section 2. We discuss in section 3 the results and limits of the PSF reconstruction method for two cases: the reconstruction on a bright reference source observed with good seeing and the reconstruction on faint sources obtained under bad seeing conditions. In section 4, we present the results of our study on the flux ratio conservation in binary systems, when using the reconstructed and an observed PSF as calibrator in deconvolution. We conclude with section 5.

2 PSF reconstruction: formalism

In this section we will give a brief description of the PSF reconstruction algorithm as it has been developed by Veran et al. ([6]) . We will use the following hypotheses:
a) long-exposure in near-field approximation, so that the optical transfer function (OTF) is given by ([5], [1]),

$$< OTF(\vec{\rho}/\lambda) >= \frac{1}{S}\int < e^{i\Phi(\vec{r})}\, e^{-i\Phi(\vec{r}+\vec{\rho})} > P(\vec{r})P(\vec{r}+\vec{\rho})\, d\vec{r}, \tag{1}$$

where $\Phi(\vec{r})$ is the residual phase, S the area of the aperture and $P(\vec{r})$ the pupil function.
b) gaussian statistics of the residual phase, which allows us to write,

$$< e^{i\Phi(\vec{r})}\, e^{-i\Phi(\vec{r}+\vec{\rho})} >= e^{-\frac{1}{2}D_{\phi}(\vec{r},\vec{\rho})}\,, \tag{2}$$

with D_Φ as the phase structure function, defined by,

$$D_\Phi(\vec{r},\vec{\rho}) =< [\Phi(\vec{r}) - \Phi(\vec{r}+\vec{\rho})]^2 > \ . \tag{3}$$

c) Kolmogorov statistics for the high spatial frequency phase.
d) Stationarity: While the structure function of a purely turbulent phase of Kolmogorov statistics is independent of $\vec{r}$, this is not true anymore for the structure function of the residual phase. However, a good approximation consists in replacing the structure function by ([1]),

$$D_\Phi(\vec{\rho}) =< D_\Phi(\vec{r},\vec{\rho}) >_r\,, \tag{4}$$

which is the structure function averaged over the pupil $P(\vec{r})$.
e) high bandwidth of the AO system, i.e. the bandwidth is higher than the cut-off frequency f_c of the highest mode corrected by the system.

With these assumptions, we can write the long-exposure optical transfer function of equation 1 as a product of three terms,

$$< OTF(\vec{\rho}/\lambda) >= OTF_{\|}(\vec{\rho}/\lambda)\, OTF_{\perp}(\vec{\rho}/\lambda)\, OTF_{sta}(\vec{\rho}/\lambda)\,, \tag{5}$$

where the first term is the OTF of the spatial low-frequency phase $\Phi_{\|}(\vec{r})$ which is partially corrected,

$$OTF_{\|}(\vec{\rho}/\lambda) = \exp[-\frac{1}{2}D_{\Phi_{\|}}(\vec{\rho})]\,. \tag{6}$$

We estimate this term from the control matrix and the covariance of the slope measurements which has to be corrected from noise contribution and the contribution of the high-frequency phase to the WFS measurements. We compute the noise on the temporal autocorrelation of the slopes ([2]). This, in principle, must be done in close loop. However, this is possible only when the correction is partial. In the case of a good wavefront correction, we calculate the noise on the open loop data which may induce some bias.

The second term is the OTF of the spatial high-frequency phase $\Phi_{\perp}(\vec{r})$ which is not corrected at all,

$$OTF_{\perp}(\vec{\rho}/\lambda) = \exp[-\frac{1}{2}D_{\Phi_{\perp}}(\vec{\rho})]\,. \tag{7}$$

We estimate this term and the contribution of the high-frequency phase to the slope measurements with a program written by F. Rigaut ([4]) which simulates an adaptive optics system in Kolmogorov turbulence. For this, we have

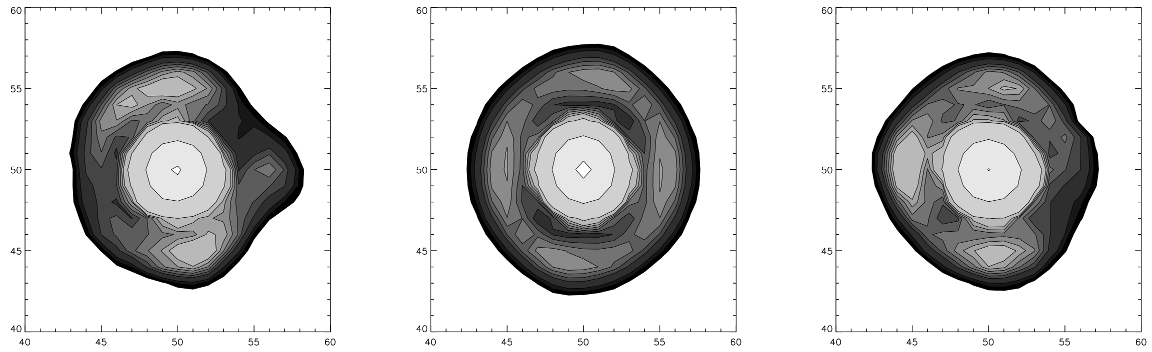

Figure 1: Contour plots of the observed PSF (left figure), its reconstructed PSF (central figure) and a second observed PSF (right figure) taken about 30 min after the first PSF. The integration time was 20 sec and the observed wavelength 2.18 μm. The visible magnitude was 7.5.

to know the parameter D/r_0 which we determine either from the variance of angle of arrival in open loop ([2]) or from the variance of the mirror commands ([6]) in close loop.

The third term is the OTF of the IR instrument which includes aberrations present in the IR channel and not corrected by the WFS.

3 PSF reconstruction: experimental results and limits

In this section, we discuss the limits of the reconstruction method in the case of a bright reference source with good seeing and faint reference sources with bad seeing. The correction on the bright PSF star was done with the RETICON WFS camera, while the EBCCD WFS camera was used in the case of the faint PSF sources.

We presented first results of the PSF reconstruction method on ADONIS in a previous paper ([3]) obtained on a bright reference source (7.5 mag) and for good seeing ($0.7''$) . In this paper, we showed the PSF reconstruction for two long-exposures taken at 2.18 μm in a narrow band filter (AO correction is at 0.6 μm). We found similar Strehl ratios of about 25 % for the reconstructed and the observed PSF with maximal differences on the spectra of about $10 - 20\%$. In Figure 1 we show the contour plots of the two observed point-like sources (left and right images) and the reconstructed PSF (central image) for the first point source.

A residual aberration is clearly seen in the case of the two observed PSFs which is not present in the image of the reconstructed PSF. This aberration which resembles a triangular coma changes in shape from one observed PSF to the other, with a correlation time of about 0.5s. It is thus reasonable to think that this aberration is due to the presence of a local turbulence which is located above the primary mirror. In this example, it is the main error source in the reconstruction method.

Recently, we reduced data taken on faint reference sources (10-13 mag) and bad seeing (~2 arcsec). The AO correction was very partial so that the Strehl ratios of the observed PSFs were between 4 and 10 %. The reconstructed OTFs are in all cases underestimated, producing Strehl ratios smaller than those for the observed ones. This is illustrated in figure 2 on a 10 mag source ($r_0 = 7.6$ and 5.7 cm respectively).

In the two examples of figure 2, the gains were high and thus the error on the reconstruction cannot be explained by a small correction bandwidth. In particular, the error is much larger on the OTF shown in the right-hand side of figure 2 for which the gains were higher than for the OTF in the left figure. For the faintest reference sources (12-13 magnitude), however, the gains were very low and may partially explain the discrepancy of the observed and estimated OTFs.

This discrepany could also be explained by a bad estimation of the noise and/or of r_0. The mean noise estimated from open loop data is about twice as high as the one determined from close loop data. Since the correction was very partial, the autocorrelation function in close loop decreases sufficiently slowly so that it is possible to estimate the noise on close loop data with an accuracy better than 10%. This uncertainty of 10% is too

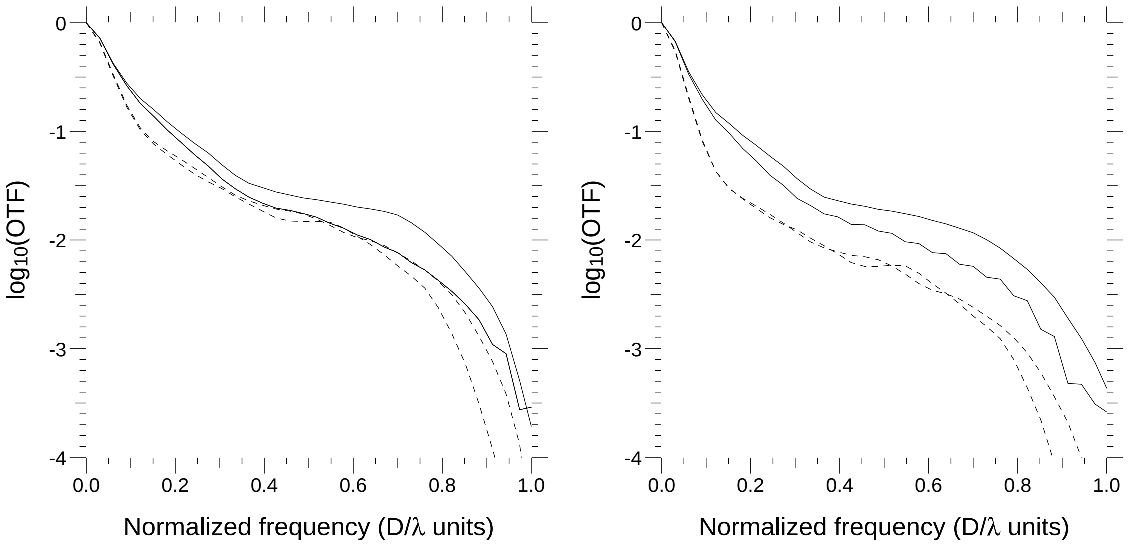

Figure 2: Two examples of the reconstructed OTF for a 10 mag reference source observed at $2.15\mu m$. The solid lines present the observed OTFs in logarithmic scale in x and y direction and the dashed lines the reconstructed OTFs. The OTF on the left-hand side was observed with $r_0 = 7.6cm$, while the OTF on the right-hand side was observed with $r_0 = 5.7cm$.

small to explain the difference of the noise in open and close loop data and it also does not explain the error on the PSF reconstruction.

To estimate the high-frequency phase structure function and the contribution of the high-frequency phase to the slope measurements, we need to know r_0. In order to explain that the reconstructed OTF is underestimated, r_0 has also to be underestimated. We compute r_0 by fitting a Noll variance to the variance of the mirror commands. A local turbulence will increase the variance of the mirror commands which will effectively lead to an underestimation of r_0. However, in the case of a very partial correction (reference source of 13 mag) the low-frequency residual phase is much more important then the high-frequency phase, so that changing r_0 even by a large factor has no effect on the reconstructed PSF.

In order to investigate the limits of the reconstruction method, we can also invoke the basic assumptions, in particular the hypothesis of stationarity. A non-stationary structure function can produce an underestimated OTF. In figure 2, the long-exposure OTF is the sum of 10 images of 10s integration time each, observed during an interval of 10 min. Since, in the reconstruction model, the OTF is calculated from the mean structure function on this cube, it may be different from the long-exposure OTF, when the structure function is not stationary. To investigate this, we calculate the structure function of a partially corrected phase by the following method. We assume that the first 50 modes are Zernicke polynomials and that the turbulence can be characterized by the Noll covariance. We then calculate the structure function for a fraction of this Noll covariance and change D/r_0 with r_0 ranging from 5 to 8.5 cm. In figure 3, we compare the mean of the exponential of the structure function times the telescope's OTF,

$$OTF_1(\vec{\rho}/\lambda) = < \exp\{-\frac{1}{2} D_{\Phi_i}(\vec{\rho})\} > OTF_{tel}(\vec{\rho}/\lambda)$$

to the exponential of the mean structure function times the telescope's OTF,

$$OTF_2(\vec{\rho}/\lambda) = \exp\{-\frac{1}{2} < D_{\Phi_i}(\vec{\rho}) >\} OTF_{tel}(\vec{\rho}/\lambda) \ .$$

One can see that $OTF_2 < OTF_1$, especially for high frequencies, with Strehl ratios of 4.9% and 6.2% respectively. This is a difference of about 20% in the Strehl ratios. However, the difference at low frequencies is much smaller than for the real case as it can be seen by comparing figure 3 with figure 2. Thus a non-stationary structure function may contribute to the error on the PSF reconstruction, but cannot fully explain it.

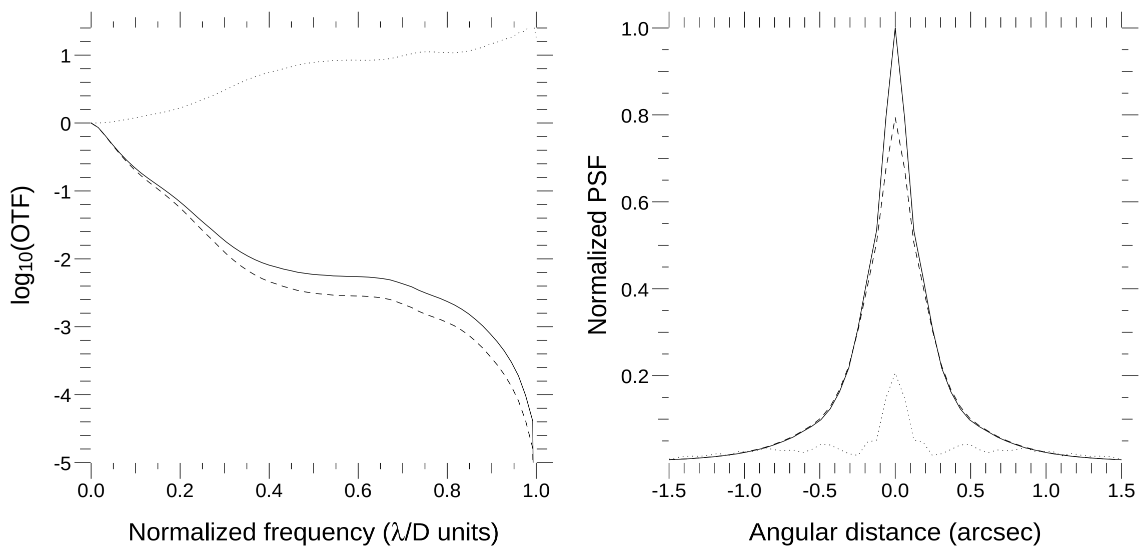

Figure 3: The continuous line in the left figure shows the average of the OTFs (OTF_1) and the dashed line the OTF of the average structure function (OTF_2), both in a logarithmic scale. The relative error (dotted line) is shown in normal scale. In the right figure are shown the corresponding PSFs both normalized to the energy of PSF_1.

We still do not have a definite explanation for the more or less large discrepancies between the reconstructed and experimental PSFs. However, in the case of a bright reference source, we showed that a variable residual aberration is present which we interpret in terms of a non-stationary local turbulence. There is *a priori* no reason for this local turbulence to have a gaussian statistics which is a basic hypothesis of the model. This can also explain, at least partially, the large discrepancies in the PSF reconstruction found for faint reference stars.

4 Flux ratio conservation in binary systems

In the case of a bright reference source, the reconstructed PSF fits quite well the observed PSF. In order to know, how accurate the reconstructed PSF is for deconvolving, we simulated a binary system by convolving two point sources with the observed PSF. We changed the separation between the sources, the position angle and the flux ratio, and deconvolved the image by the reconstructed PSF. For this, we use the Lucy-Richardson algorithm. We determined the flux ratio by integrating the flux on a square around each point source. We preferred this method instead of fitting two gaussian functions to the sources, because the two sources are well separated after deconvolving and integrating over a region is less sensitive to the exact form of the image profiles.

Figure 4 shows the relative error on the flux ratio estimate versus separation for all 4 flux ratios (filled circles). In the left top figure which presents the case of $\Delta F = 1$ it can be seen that the mean relative error is about 2 %. For $\Delta F = 2$ which is shown in the right top graph, it is 3 % and for $\Delta F = 4$ (left bottom) it becomes 7 %. For $\Delta F = 10$ (right bottom) the mean relative error is about 25 %. In all four cases the sigma on the relative error is about the same as its average value.

We also deconvolved the images with the second observed PSF in order to compare the calibration by the reconstructed and an observed PSF. The results we found are similar to the case of the reconstructed PSF and are also shown in figure 4 (open circles). The error on the flux ratio comes in both cases essentially from the differences at the location of the first diffraction ring as it can be seen in figure 1 and in figure 5. This explains that the relative error is strongest for a distance typically twice the radius of the first diffraction minima.

The results of this simulation show that the photometric accuracy on a double system will not be better than 5-10% for flux ratios less than 4 due to the presence of a residual non-stationary aberration. This is true when deconvolving the image by the reconstructed PSF as well as by an observed PSF. Thus it will be difficult to calibrate accurately images obtained with the adaptive optics system ADONIS, as long as this aberration has not been removed.

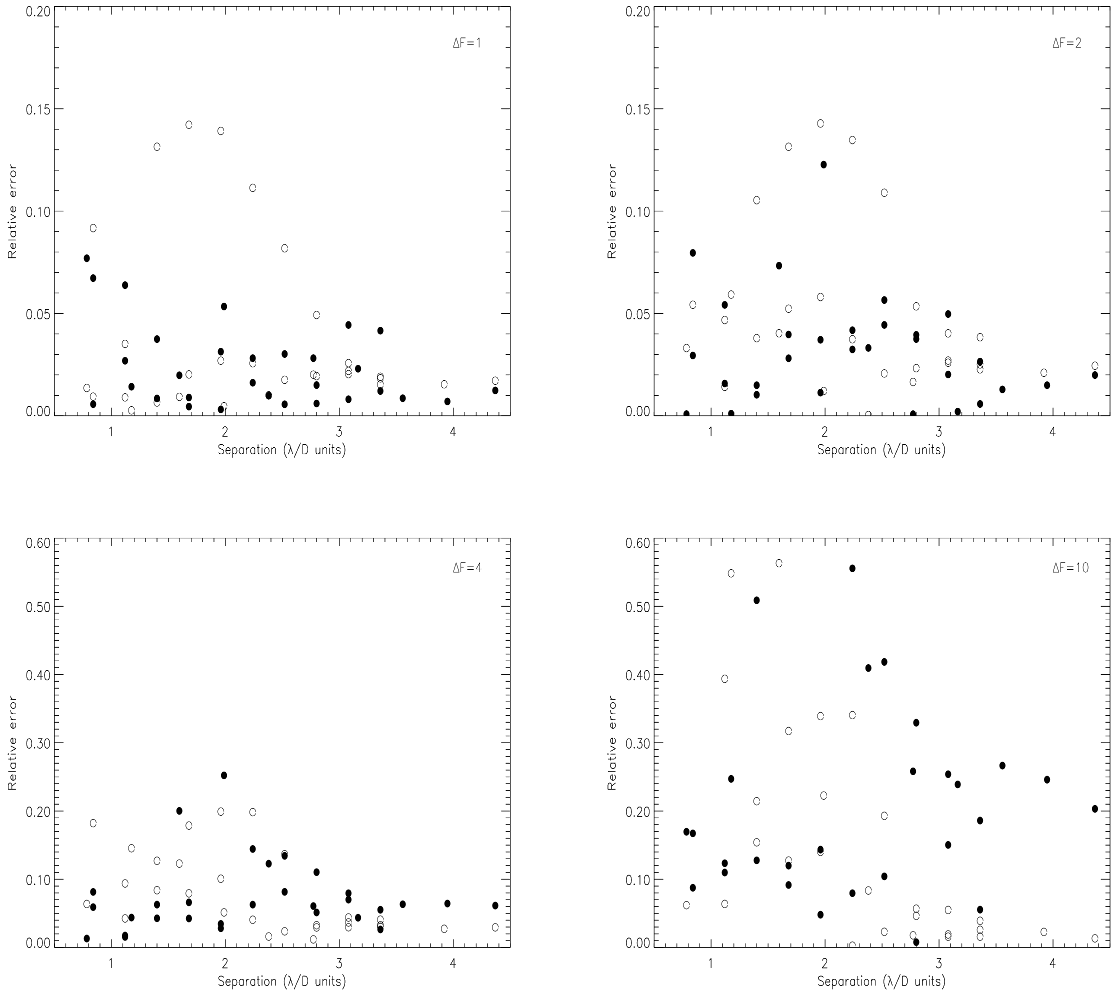

Figure 4: Relative error on the flux ratio estimate versus separation (in λ/D units) for flux ratios ΔF =1, 2, 4 and 10. The filled circles present the result of the deconvolution by the reconstructed PSF and the open circles the result of deconvolution by a second observed PSF.

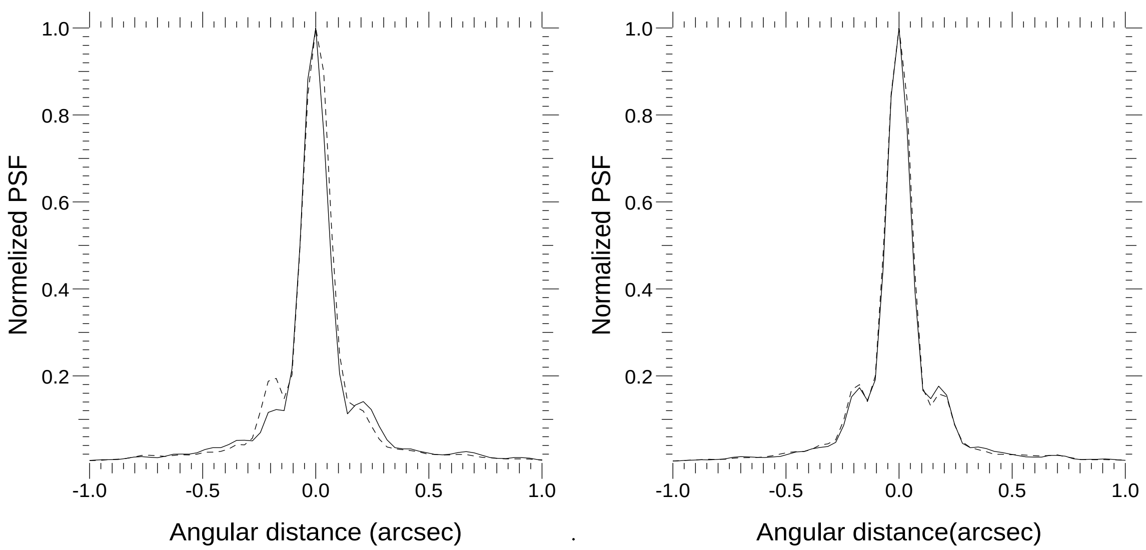

Figure 5: 2 bright reference sources (same as in fig.1), the continuous lines present the first PSF, while the dashed lines present the second PSF taken 30 min later. The left figure shows the x-cut of the PSFs and he right figure the y-cut. A large difference between the PSFs on the first diffraction ring can be seen in left figure.

Figure 6 summarizes the results by showing the mean relative error on the flux ratio estimate versus the flux ratio.

5 Conclusion

We have discussed the limits of the current PSF reconstruction method for the adaptive optics system ADONIS on the example of a bright reference source observed with good seeing and on faint reference stars obtained with bad seeing. In the first case, the main source of error is the presence of a residual aberration. This aberration has the shape of a triangular coma and is variable in time. Since it is difficult to imagine how an atmospheric turbulence may create a non-stationary aberration with a large correlation time (0.5s), we think that it is due to a non-stationary local turbulence, probably situated above the primary mirror.

For the data obtained with bad seeing, the reconstructed OTF is always underestimated, at low and high frequencies. We found that an inaccurate estimation of the noise and of r_0 cannot explain the large discrepancy between observed and estimated OTFs. It could be due to the presence of a local turbulence, but a non-stationary structure function may also contribute to the error on the PSF reconstruction. However, we still do not fully understand this large error.

In the case of a bright reference source, we have shown that the accuracy on the flux ratio calculation of a binary system is about 5-10% for flux ratios less than 4 due to the presence of the variable residual aberration. We have found the same result, when deconvolving the binary system with the reconstructed PSF as well when deconvolving it with an observed PSF.

The non-stationary residual aberration sets an ultimate limit to the PSF reconstruction, but also limits the calibration by an observed PSF. For this reason, its cause has to be found and removed. Otherwise, it will be difficult to do very precise photometry with ADONIS. Additional observations of reference stars under different observing conditions are necessary to determine the domain of the validity of our PSF reconstruction method and to investigate the importance of the residual aberration.

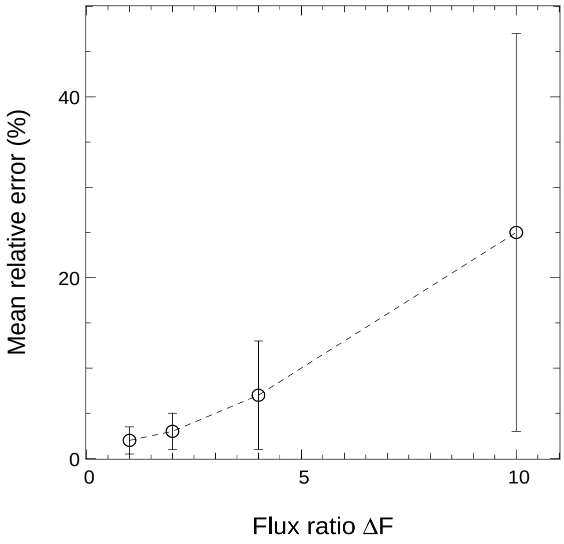

Figure 6: Mean relative error on the flux ratio estimate versus flux ratio.

References

[1] Conan, J.M., *Étude de la correction partielle en optique adaptative*, PhD thesis, Université Paris XI, Orsay, Paris, 1995

[2] Gendron, E. & Léna, P., "Astronomical adaptive optics II: experimental results of an optimized modal control", Astron. Astrophys. Suppl. Ser., 111, pp 153-167, 1995

[3] Harder, S., Chelli,A., "Estimation of the point spread function for the adaptive optics system ADONIS", in *Adaptive Optical System Technologies*, vol. 3353 of proc SPIE, 1998

[4] Rigaut F., Arsenault, R., Kerr, J., Salmon, D., Northcott, N., Dutil, Y., Boyer, C., "The Canada-France-Hawaii adaptive optics bonnette II: simulations and control", in *Adaptive Optics with Astronomy*, vol. 2201 of proc. SPIE, 1994

[5] Roddier, F., "The effect of atmospheric turbulence in optical astronomy", in *Progress in optics*, volume XIX, E. Wolf, ed., pp. 281-376, North-Holland, Amsterdam, 1981

[6] Véran, J.P., Rigaut, F., Maître H., Rouan D., "Estimation of the adaptive optics long exposure point spread function using control loop data", J. Opt. Soc. Am. A, 14(11), 1997